East African Journal of Engineering
eaje.eanso.org
Volume 7, Issue 1, 2024
Print ISSN: 2707-5389 | Online ISSN: 2707-5397
Title DOI: https://doi.org/10.37284/2707-5397
EAST AFRICAN NATURE & SCIENCE ORGANIZATION

Original Article

Analytical Design of a Portable Surface Plasmon Resonance Sensor by Using a Divergence Beam for Measuring Multiple Heavy Metals and Other Contamination Simultaneously

Jordan H. Hossea[1] & Georgia Rugumira[1]*

[1] Dar es Salaam Institute of Technology, P. O. Box 2958, Dar es Salaam, Tanzania.
* Author for Correspondence ORCID ID: https://orcid.org/0000-0002-1224-8842; Email: jordan.hossea@dit.ac.tz

Article DOI : https://doi.org/10.37284/eaje.7.1.1967

Publication Date:

04 June 2024

Keywords:

Divergence Beam, SPR Sensor, Multiple Heavy Metal Ion

ABSTRACT

The study proposes a surface plasmon resonance (SPR) sensor for measuring water quality by detecting the presence of heavy metal ions and other contamination. The proposed SPR sensor operates in the Kretschmann configuration, which employs the divergence beam produced by the Powell lens. The beam is diverged to eliminate mechanical scanning, indicating that the sensor can measure water quality from deionized water (DIW) with refractive index (RI) of 1.3317, diluted DIW with multiple heavy metal ion such as Hg[II], Pb[II], Ni[II], Zn[II], Cu[II] at concentration of 100 µM and other pollutant with the RI of 1.34 without any mechanical movement. The proposed SPR sensor has a theoretical sensitivity of 399.45°/RIU and resolution of 1.3456×10-8 and 8.3790×10-10RIU with 8-bits (ATmega1284) and 12-bits (STM32F401RE) ADC of the controller, respectively. The CCD sensor (TCD1304AP) and microcontroller data sheets were used to calculate the theoretical in which all these components are very chip. The reported sensitivity and resolution were achieved because of the proper application and optimization of TiO2 and BaTiO3. In comparison to a conventional SPR sensor, the proposed SPR improved sensitivity and figure of merits by 50.98 % and 13.93 %, respectively. Furthermore, the proposed SPR sensor outperforms recently published research in terms of performance.

APA CITATION

Hossea J. H. & Rugumira G. (2024). Analytical Design of a Portable Surface Plasmon Resonance Sensor by Using a Divergence Beam for Measuring Multiple Heavy Metals and Other Contamination Simultaneously *East African Journal of Engineering*, 7(1), 148-161. https://doi.org/10.37284/eaje.7.1.1967

CHICAGO CITATION

Hossea, Jordan H. and Georgia Rugumira. 2024. "Analytical Design of a Portable Surface Plasmon Resonance Sensor by Using a Divergence Beam for Measuring Multiple Heavy Metals and Other Contamination Simultaneously". *East African Journal of Engineering* 7 (1), 148-161. https://doi.org/10.37284/eaje.7.1.1967.

HARVARD CITATION

Hossea J. H. & Rugumira G. (2024) "Analytical Design of a Portable Surface Plasmon Resonance Sensor by Using a Divergence Beam for Measuring Multiple Heavy Metals and Other Contamination Simultaneously", *East African Journal of Engineering*, 7(1), pp. 148-161. doi: 10.37284/eaje.7.1.1967.

IEEE CITATION

J. H., Hossea & G., Rugumira "Analytical Design of a Portable Surface Plasmon Resonance Sensor by Using a Divergence Beam for Measuring Multiple Heavy Metals and Other Contamination Simultaneously" *EAJE*, vol. 7, no. 1, pp 148-161, Jun. 2024.

Article DOI: https://doi.org/10.37284/eaje.7.1.1967

MLA CITATION

Hossea, Jordan H. & Georgia Rugumira. "Analytical Design of a Portable Surface Plasmon Resonance Sensor by Using a Divergence Beam for Measuring Multiple Heavy Metals and Other Contamination Simultaneously." *East African Journal of Engineering*, Vol. 7, no. 1, Jun. 2024, pp. 148-161, doi:10.37284/eaje.7.1.1967.

INTRODUCTION

According to a water organization study, 16 million Tanzanians (28% of the population) lack access to safe water, and 44 million Tanzanians (73%) lack access to safely managed household sanitation facilities [1]. The definition of safely managed water is a water source that is close to living premises, is available when needed, and is free of faecal and chemical contamination.

The consumed water is generated from water from surface sources such as rivers, streams, shallow and deep wells. These sources of water can be contaminated in various ways such as industrial activities like chemicals, metals, and organic substances into water bodies, which can cause severe water pollution. Furthermore, agricultural activities like farming, irrigation, livestock rearing, use of fertilizers, pesticides, and herbicides, can find their way into water sources through runoff and leaching. These chemicals can cause eutrophication, the growth of harmful algae, and contamination of drinking water. Besides that, improper disposal of sewage and wastewater can also lead to water pollution by introducing heavy metals. Untreated or partially treated wastewater contains high levels of nutrients, organic matter, and pathogens, which can harm aquatic life and human health. For example, a study conducted by Machiwa found that during the rainy season, all the waste material from industries and construction is directed to the sea through the Msimbazi River without any treatment which increases the contamination of the sea. Machiwa's works identified the presence of heavy metals in the coastal water. The findings observed that the water near the Dar es Salaam harbour is highly contaminated with cadmium (Cd) and chromium (Cr), while the areas of the harbour are highly contaminated with iron (Fe) and lead (Pb). Due to an increase in heavy metal pollution in Dar es Salaam's harbour, which can be carried by sea fish, which is directly consumed by people [2]. The consumption of heavy metal ion water, an ineffective sanitation system and improper handling of non-piped water supply systems are the main causes of severe headaches, cancer, diarrhoea, cholera, dysentery, and typhoid [3, 4]

The government maintains a policy that ensures the company follows the regulation of pre-treating garbage before disposing it into the seas. Furthermore, the government emphasizes educating the public on basic hygiene principles such as the use of pit latrines and boiling drinking water. Boiling or chemically treating water can only kill microorganisms but cannot obviate heavy metals such as mercury ions, lead ions, and copper ions.

Due to budget constraints, the Tanzanian government has set a 2% target for water supply, sewerage, and waste management [5]. Aside from budget constraints, the existing instruments for testing the quality of water supply are few and laboratory-based equipment. Poor sewage and waste pre-treatment management are among the contributing factors for contaminating the sea with heavy ion metal.

Conventional measurement instruments used by researchers to detect the quality of water by measuring the presence of heavy metals and other contamination are i) atomic absorption spectroscopy (AAS) [6] and ii) inductively coupled plasma mass spectroscopy (ICP-MS) [7]. However, these instruments have the demerits of requiring sample pretreatment which makes them unsuitable for real-time water sample measurement and having complex detection mechanisms which require skilled personnel to interpret the results [8, 9]. Electrochemical impedance spectroscopy, voltammetry and polarography [10], and UV-visible spectrophotometer, also these devices has low detection accuracy in differentiating metal ions whose structure radii appear uniformly [11]. Another common method of measuring metal ions in water is the chemiluminescence method which

Article DOI: https://doi.org/10.37284/eaje.7.1.1967

is not suitable for measuring low concentration [12]. A common method is an electrochemical method, which uses chemical pretreatment of the sample to improve its ability to detect low concentrations of heavy metal ions in the wate r[13]. The effect of adding chemicals to the sample is the possibility of causing the secondary contamination [13]. **In summary, the mentioned measurement instruments are too expensive for developing countries like Tanzania to purchase and operate. Furthermore, they are bulky and laboratory-based which is unsuitable for online heavy metal ion and other contamination monitoring in the drinking water.**

An alternative approach of using the surface plasmon resonance (SPR) technique was proposed. Since the SPR sensors were discovered, the technique has been applied to the detection of bacteria [14, 15] and coronavirus [16], the detection of adulteration of honey [17, 18] and milky [19-21] and measuring the quality of food [22]. In addition, SPR sensors were applied to measure heavy metal ions in the water [4, 23-28]. Most of the proposed methods were able to detect one type of heavy metal ion at a time. Additionally were have very low sensitivity because they use convectional Kretschmann configuration, the prism with a high refractive index 1.7786 and it requires mechanical scanning to measure more than one heavy metal ion and other contaminant in water [23, 27]

Therefore, the goal of this research work is to perform an analytical analysis of the SPR-based optical instrument which was applied in measuring multiple heavy metal ions (Hg [II], Pb [II], Ni [II], Zn [II], Cu [II]) and other contamination simultaneously without mechanical scanning. The theoretical performance in measuring the minimum concentration of heavy metal ions and other contaminations present in the water solution was evaluated. Despite the commercial availability of some SPR-based biosensing instruments such as Biacore, Spreeta, Reichert, Bruker, Texas Instrument, Plasmetrix, and Biorad, which have high sensitivity and stability, making them ideal for biomolecule analysis and they can also be customized for quantifying heavy metal ion and other water contamination; however, they are very expensive and require a compatible accessory, which is also costly. They also require skilled personnel and have a high operational cost.

Since heavy metal ions cannot be eliminated by boiling water or well-cooking seafood thus, in such a scenario, there is a need to design a portable SPR sensor which is easy to use, low-cost, portable, and high-sensitivity instrument.

METHODOLOGY

Theory and Mathematical Modelling of SPR Sensor

The wave vector of the generated evanescent wave along the horizontal axis can be expressed as

$$K_x = \frac{2\pi}{\lambda} n_p \sin\theta_i \qquad (1)$$

where n_p is the prism RI.

Figure 1: Conventional SPR sensor.

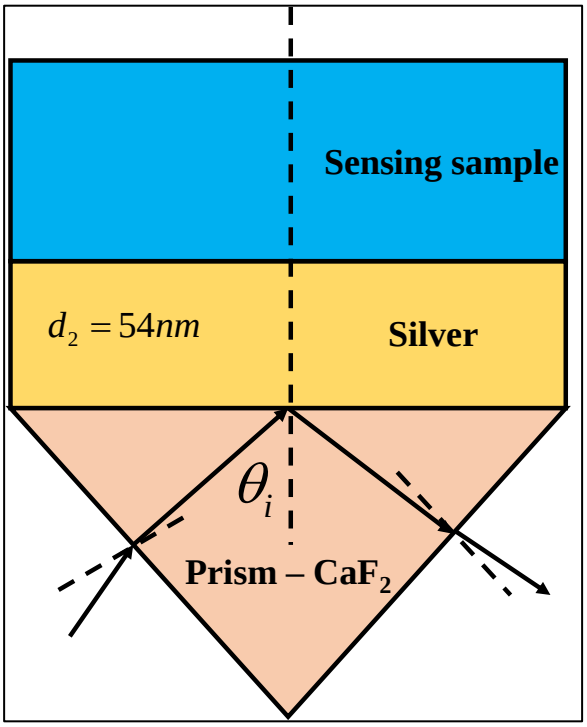

Article DOI: https://doi.org/10.37284/eaje.7.1.1967

When there is an oscillation of surface charges on the silver layer, the surface plasmon wave vector K_{sp} [29] can be expressed as

$$K_{sp} = \frac{2\pi}{\lambda}\sqrt{\frac{n_{silver}^2 n_{sample}^2}{n_{silver}^2 + n_{sample}^2}}, \qquad (2)$$

Here, n_{silver}, n_{sample} are the refractive indices of the silver and dielectric samples, respectively. Thus, Eq (2) demonstrates that changes in refractive index affect the horizontal wave vector of metal oscillating electron charges.

The perturbation K_{sp} in the presence of the prism gives K_p [30]

$$K_p = K_{sp}\left(\frac{2}{n_{silver}^2 + n_{sample}^2}\right)\sqrt{\left(\frac{n_{silver}^2 n_{sample}^2}{n_{silver}^2 + n_{sample}^2}\right)^3}\exp\left(i\frac{4\pi d_{silver}}{\lambda}\left(\frac{n_{silver}^2}{\sqrt{n_{silver}^2 + n_{sample}^2}}\right)\right) \qquad (3)$$

where d_{silver} is the thickness of the silver layer. Thus, the total wave vector K is given as a summation of the surface plasmon wave vector K_{sp} and perturbed wave vector K_p

$$K = K_{sp}\left[1 + K_p\right] \qquad (4)$$

The two wave vectors must match in order for the plasmons to resonate, yielding the resonance angle of

$$\theta_{spr} = \sin^{-1}\left[\frac{1}{n_p}\sqrt{\frac{n_{silver}^2 n_{sample}^2}{\left(n_{sillver}^2 + n_{sample}^2\right)}}\right] \qquad (5)$$

SPR Sensor Design, Mathematical Modelling, And Optimization

SPR Sensor Model Design

Figure 2 illustrates a four-layer structure of the SPR when the p-polarized light with wavelength λ (632.8 nm) incident on the prism. To avoid mechanical translation or movement, the collimated source is passed through the Powell lens which diverges the laser beam to ensure that the beam incident on the prism-TiO_2 interface covers the measurement range of the RI from 1.3317 to 1.34. The modified structure of the SPR sensor is proposed by stacking the layers of the dissimilar materials on the z-axis. These works choose the CaF_2 prism has a refractive index of 1.4329 which is smaller than BK7 and FK51a with a refractive index of 1.5151 and 1.4853, respectively. It proven that the SPR sensor which uses the prism with low RI has higher sensitivity. The stacked layers consist of CaF_2/TiO_2/Silver/$BaTiO_3$/sensing sample as shown in *Figure 2*. In which the prism, TiO_2, silver $BaTiO_3$, and sensing sample are the four layers that make up the proposed SPR sensor. While $BaTiO_3$ is added to increase sensitivity and reduce the impact of oxidation, TiO_2 is added to ensure that the silver is firmly connected to the prism and to increase figure of merit (FOM) [31]. *Table 1* shows optical and physical parameters used in the designing of the proposed SPR sensor.

The reflected beam from prism – TiO_2 interface is reflected to other side of the prism. Therefore, the reflected intensity can be monitored by a charge couple device (CCD).

Detection of Heavy Metal Ion

The study uses the data published in the paper [32] for validating the performance the designed SPR sensor in detecting deionized water contaminated with the concentration of 100 μM the heavy metal ions. The study focuses not only on detecting contaminated water polluted by heavy metal ions and other pollutants which extends the RI of the diluted DIW to 1.34. *Table 2* illustrates the refractive index of heavy metal ion polluted water at a concentration of 100 μM, with nickel ion having a high RI of 1.333034, which is within the SPR sensor's measurement range. Meanwhile, water contaminated with other heavy metals has a lower RI than water contaminated with nickel ions.

Article DOI: https://doi.org/10.37284/eaje.7.1.1967

Figure 2: Proposed a four-layer SPR sensor.

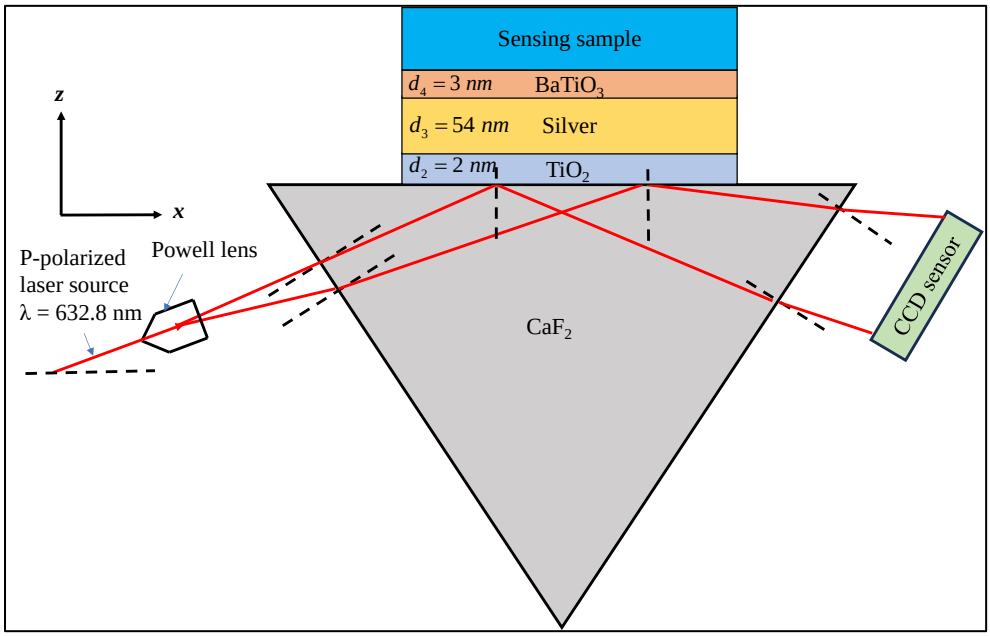

Table 1: optical and physical parameters used in the designing of the proposed SPR sensor.

Number of layers	Used material	The refractive index of the material at 632.8 nm	Thickness (nm)
1	Prism (CaF_2)	1.4329	-
2	TiO_2	2.5837	$d_2 = 2$
3	Silver	0.05626+4.2776i	$d_3 = 54$
4	$BaTiO_3$	2.4042	$d_4 = 3$
5	Sensing sample	1.3317 – 1.34	-

Table 2: Metal ion solution refractive indices [32]

S. No	The concentration of each metal ion was 100 µM in water [32].	RI of contaminated water with heavy metal
1	Hg[II]	1.332889 ± 0.0000065
2	Pb[II]	1.333284 ± 0.0000123
3	Ni[II]	1.333034 ± 0.0000184
4	Zn[II]	1.332842 ± 0.0000124
5	Cu[II]	1.332907 ± 0.0000172

SPR Sensor Mathematical Modelling

The SPR reflectivity curve was calculated in this study using the matrix method [33] on MATLAB software. According to the boundary condition, the electric and magnetic fields, U1 and V1, at the first layer's boundary are related to those U4 and V4 at the last layer's interface, respectively, by

$$\begin{bmatrix} U_1 \\ V_1 \end{bmatrix} = M \begin{bmatrix} U_4 \\ V_4 \end{bmatrix} \quad (6)$$

where M is the matrix representing the wave propagation response through different layers by

$$M_{ij} = \prod_{k=2}^{4} \begin{pmatrix} \cos\beta_k & -(i/q_k)\sin\beta_k \\ -iq_k \sin\beta_k & \cos\beta_k \end{pmatrix}_{ij} = \begin{pmatrix} M_{11} & M_{12} \\ M_{21} & M_{22} \end{pmatrix}. \quad (7)$$

Here, the factor q_k is defined as

$$q_k = \frac{\left(n_k^2 - \left(n_p \sin\beta_i\right)^2\right)^{1/2}}{n_k^2}, \quad (8)$$

Article DOI: https://doi.org/10.37284/eaje.7.1.1967

while β_k is the phase shift of k^{th} layer with a thickness d_k

$$\beta_k = \frac{2\pi d_k}{\lambda}\left(n_k^2 - n_p^2 \sin^2\theta_i\right)^{1/2} \quad (9)$$

As the result of the wave propagation through multilayer media, the total reflection coefficient for the transverse magnetic field is expressed by

$$r^{TM} = \frac{\left(M_{11} + M_{12}q_{sample}\right)q_1 - \left(M_{21} + M_{22}q_{sample}\right)}{\left(M_{11} + M_{12}q_{sample}\right)q_1 + \left(M_{21} + M_{22}q_{sample}\right)} \quad (10)$$

with

$$q_{sample} = \frac{\left(n_{sample}^2 - \left(n_p \sin\theta_i\right)^2\right)^{1/2}}{n_{sample}^2} . \quad (11)$$

Finally, the reflectivity power can be calculated as

$$R = \left|r^{TM}\right|^2 . \quad (12)$$

The SPR Sensor Measurement Parameters

The SPR sensor measurement parameters were extracted from the resonance curve, in which sensitivity, detection accuracy and quality factor.

Sensitivity

Sensitivity of the SPR biosensor is measured as change in resonance position in the reflectance curve ($\Delta\theta res$) corresponding to the small change in the refractive index (Δns) of the analyte. The sensitivity(S) is given by,

$$S = \frac{\Delta\theta_{res}}{\Delta n_s} \quad (13)$$

Detection Accuracy (DA)

DA is inversely proportional to the full width at half maximum (FWHM) of the reflectance curve and is given by,

$$DA = \frac{1}{FWHM} \quad (14)$$

Quality Factor (Q) or Figure of Merits (FOM)

The quality factor of the SPR sensor depends on the sensitivity and FWHM [31]. This implies that the higher the quality the better signal to noise ratio. Therefore, the quality factor (Q) is given the product of the detection accuracy (DA) and the sensitivity S,

$$Q = S.DA \quad (15)$$

Resolution of the Proposed SPR Sensor

Resolution $\left(\sigma_{RI}\right)$ is the least change of RI that produced detectable output response, which can be expressed as below.

$$\sigma_{RI} = \frac{\sigma_s}{Sensitivity} \quad (16)$$

RESULTS AND DISCUSSION

Optimization of Metal Thickness

The critical factor ensuring the photon energy is transformed into the surface plasmon wave is the thickness of the metal layer. The metal's optimum thickness ensures that at resonance, all the photon energies are converted to plasmon energy. With a sensing sample of 1.3317 for pure water and 1.34 for contaminated water samples, the thickness of the silver was opted from 44 and 56 nm (see *Figure 3*).

Figure 1 demonstrates that the minimum dip occurred when the thickness of the silver was 44 nm, indicating an energy transfer efficiency of 80%. The energy transfer efficiency is decreased because of the strong evanescent field at silver/sample which fraction of it is coupled with few surface plasmons while excess photon energy will be reflected to the detector. Similarly, when the silver thickness is 56 nm the minimal dip increases to 0.02 and the energy transfer efficiency rises to 99.98%. Thus, the reduction of the minimum dip is a resulted of the weak evanescent field arriving at the silver/sample interface hence less evanescent energy can interact with surface plasmon. However, the minimum dip is almost zero and the energy

Article DOI: https://doi.org/10.37284/eaje.7.1.1967

transfer efficiency is close to 100% when the metal thickness is 54 nm.

The ideal thickness of the silver is beneficial in ensuring sufficient photon energy reaches the interface between the silver/sample. It also simplifies the algorithm of detecting the minimum dip using a straightforward technique. The silver film thickness was chosen to be 54 nm for the theoretical analysis study because it provides the best coupling between photon energy and plasmon energy at resonance.

Figure 3: SPR reflectivity curve for silver thickness optimization

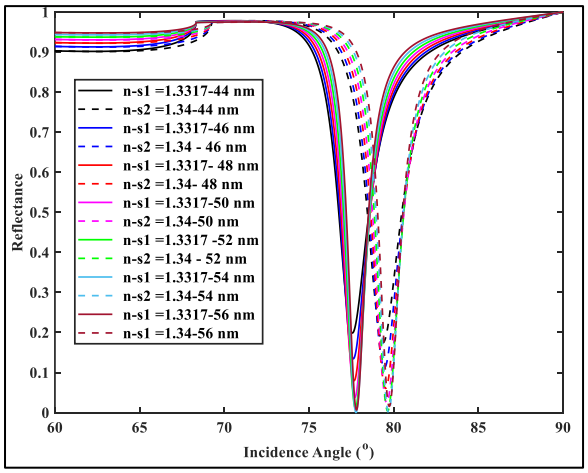

The reflectance curve for a traditional SPR sensor is shown in *Figure 4*. Prism, silver, and the sensing sample are the only layers in a conventional SPR sensor. Pure water in the detecting sample has a RI of 1.3317, but contaminated water with other pollutants has a RI of 1.34. As can be observed in *Figure 4*, when the water's RI is increased to 1.34, the resonance position changes by 1.921˚ while the RI changes by 0.0038. The fullwidth at half maximum (FWHM) parameter controls the SPR sensor's accuracy, the higher the detection accuracy, the narrower the reflectivity.

The convection SPR sensor's FWHM is 1.433˚. As a result, the conventional SPR sensor has a theoretical sensitivity, detection accuracy (DA), and quality factor (Q) of 231.45 ˚/RIU, 1/1.433 = 0.7/˚, and 231.45/1.433 = 161.5 /RIU, respectively.

Figure 4: SPR reflectivity curves for a conventional SPR sensor

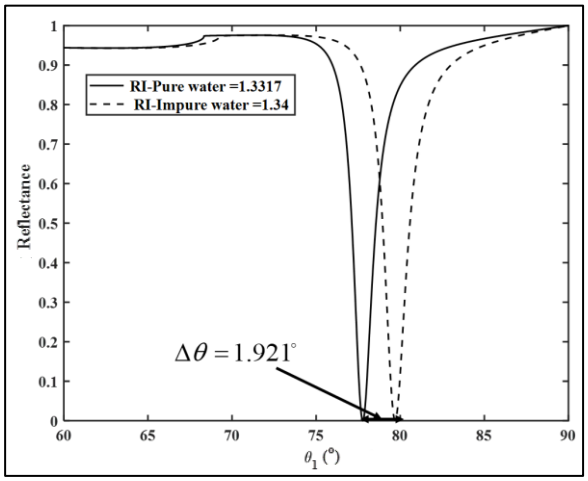

The reflectance curve in *Figure 5* indicates simulated results for the proposed SPR sensor. Also, *Figure 5* shows that as RI of the sample increases because of the contamination of deionized water (DIW) being diluted with multiple heavy metal ions at the concentration of 100 μM, the resonance dip shifts toward a higher resonance position. It is anticipated that the proposed SPR sensor outperforms the convectional SPR sensors in terms of sensitivity. As seen in *Figure 5*, when the water's RI is increased to 1.34, the resonance position changes by 3.255 while the RI changes by 0.0083 while *Figure 4* gives the resonance shift of 1.921 at the same change in RI, which implies noticeable improvement as the results of adding TiO_2 and $BaTiO_3$.

Figure 5: SPR reflectivity curves for a proposed SPR sensor

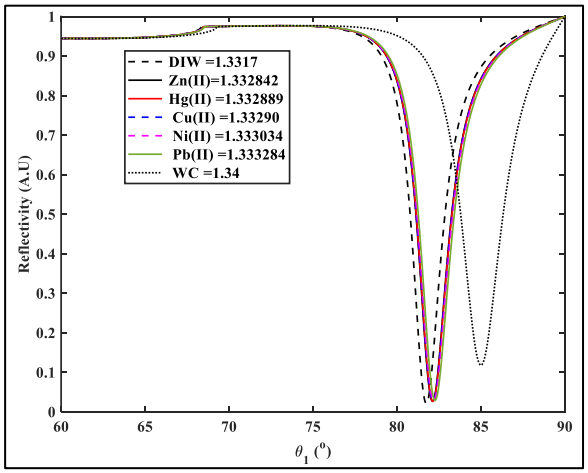

Article DOI: https://doi.org/10.37284/eaje.7.1.1967

Sensitivity

Figure 6 summarizes the resonance angle as the function of the RI of the DIW, and DIW diluted with Hg[II], Pb[II], Ni[II], Zn[II], Cu[II] at a concentration of 100 μM and when it is contaminated with other impurities that give rise to 1.34. Because the range of the RI of the sample is wide, we extracted the data from *Figure 6*, applied the linear regression analysis and found that RI correlated with resonance angle by 0.999 with linear equation of $\theta_{\text{Resonance}} = 399.448509RI - 450.273045$. The slope of *Figure 6* implies the sensitivity of the proposed SPR sensor which is 399.45˚/RIU

Figure 6: SPR sensor sensitivity analysis

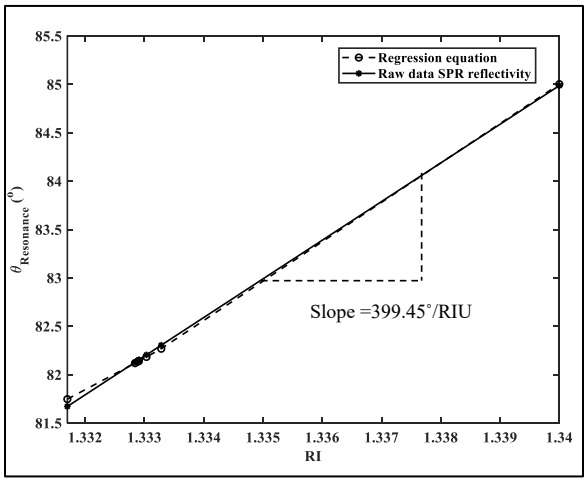

The full width at half maximum (FWHM) and detection accuracy

The full width at half maximum (FWHM) is the parameter that governs the SPR sensor's accuracy, the higher the detection accuracy, the narrower the reflectivity. Mathematical expressed as

$$FWHM = \frac{2im(K)}{k_0 n_p \cos\theta_{spr}} \qquad (17)$$

Equation (17) signifies that the resonance angle increases the FWHM. *Figure 7* shows as RI of the sample increases FWHM increases. This can be explained theoretically because FWHM is inversely proportional to the cosine of the resonance angle refer Eq (1) and Eq (17). The proposed SPR sensor has an average FWHM of 2.1710. Therefore, the detection accuracy (DA), and quality factor for the proposed SPR are each calculated as follows: 399.45/2.171 = 183.9936 /RIU, 1/ (2.171) = 0.4606, respectively. The proposed SPR sensor has improved sensitivity and quality factor over the convectional SPR sensor by 118 /RIU and 22.4936 /RIU, respectively, while the detection accuracy is decreased by 0.2394 which is caused by the broadening reflectivity curve due addition of $BaTiO_3$ which causes backscattered photon field to increase hence radiation damping. In summary, the proposed SPR sensor outperformed the convectional SPR sensor in terms of sensitivity and quality factor or figure of merits by 50.98 % and 13.93 %, respectively. Meanwhile, the detection accuracy has lowered by 34.2 %. Even though the detection accuracy is an important parameter in the SPR sensor, for heavy metal ion detection in water, the important parameter is sensitivity.

Figure 7: FWHM for a proposed SPR sensor

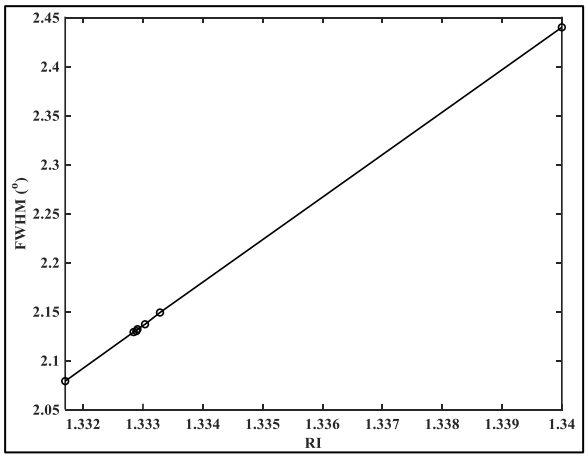

Minimum Dip

The minimum dip is shallow as the level of contamination increases as shown in *Figure 8***.** This implies the energy transfer efficiency is decreasing as RI of the samples is increasing. This happens because as the resonance angle increases because of water contamination, less photon energy is transferred to the silver/sample interface which resulting less photon energy is interacted with the plasmon energy.

Article DOI: https://doi.org/10.37284/eaje.7.1.1967

Figure 8: Minimum dip for a proposed SPR sensor

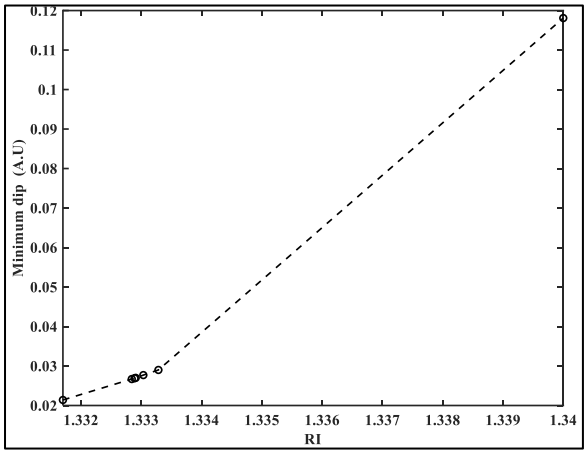

Resolution of the Proposed SPR Sensor

The use imbedded linear array TCD1304AP CCD which is very cheap with 3648 pixels. The controller for the CCD sensor is two types of controllers which are ATmega1284 and STM32F401RE microcontroller used as the controller with 8-bit ADC converter. While STM32F401RE is the controller with 12-bit ADC converter. The designed SPR sensor used a simple and tiny CCD sensor which contributes to a portable and cheap SPR sensor. The theoretical resolution of the proposed SPR sensor can be estimated according to the theorem presented in []. The range of the resonance angle is 5˚ which means from 81 to 86˚ as shown in *Figure 6*

$$\sigma_{RI} = \frac{\sigma_s}{Sensitivity} \tag{18}$$

Where σ_s is the output noise fluctuations level. σ_s depends on the pixel range covered by resonance angle and the ADC conversion resolution $1/\left(2^n - 1\right)$ is multiplied by the resolution of the CCD. The resolution of the CCD sensor is the minimum angle at which CCD sensor can track changes in one pixel.

$$\sigma_s = \frac{\Delta\theta_{res}}{T_{pixel}} \times \frac{1 pixel}{\left(2^n - 1\right)} \tag{19}$$

Case 1, ATmega1284 controller with 8-bit ADC converter

$$\sigma_s = \frac{5^\circ}{3648 pixel} \times \frac{1 pixel}{255} = \frac{5^\circ}{930240} = 0.000005375^\circ \tag{20a}$$

$$\sigma_{RI} = \frac{5.375 \times 10^{-6\circ}}{399.45^\circ / RIU} = 1.3456 \times 10^{-8} RIU \tag{20b}$$

Case 2, STM32F401RE controller with 12-bit ADC converter

$$\sigma_s = \frac{5^\circ}{3648 pixel} \times \frac{1 pixel}{4095} = \frac{5^\circ}{14938560} = 3.3470 \times 10^{-7\circ} \tag{21a}$$

$$\sigma_{RI} = \frac{3.3470 \times 10^{-7\circ}}{399.45^\circ / RIU} = 8.3790 \times 10^{-10} RIU \tag{21b}$$

Comparison of the Proposed SPR Sensor with Other Published Work

Table 3 compares the performance of proposed SPR sensors to previously published work. The results show that the proposed SPR sensor exceeds prior studies in terms of sensitivity and quality factor, both of which are crucial characteristics in detecting heavy metal ions in wate.

Article DOI: https://doi.org/10.37284/eaje.7.1.1967

Table 3: Comparison with recently published studies.

References	λ (nm)	Structures	Sensitivity (˚/RIU)	Detection Accuracy DA (/˚)	Quality factor (/RIU)
Abassi et al 2021 [34]	633	Ag-TiO2-MAPbBr3-Graphene	255.80	0.492	126.00
[14]		BK7–Ag–BaTiO3-Graphene-Affinity-Sensing layer	220		101.38
[35]	633	CaF2–ZnO–Ag–BaTiO3-BlueP/WS2-Affinity-Sensing layer	343.51		
[36]		BK7–ZnO–Ag–BaTiO3–graphene	157		
[37]		BK7–Ag–BaTiO3–graphene	257		
	633	Ag - BaTiO3 – graphene - affinity layer	220	7.09	101.38
[36]		BK–Ag–BaTiO3–graphene	302	Fwhm(7.1)	
Karki et al. 2022 [38]	633	Au – ε-Tin selenide – Au - Graphene	214	0.487	26.9
[39]	633	BK7-Ag-Si-BaTiO3-BP-Affinity-Sensing layer	370		86.65
Sharma et al 2022 [40]	633	Ag-$BaTiO_3$-MXene	316	0.3072	97.075
Proposed SPR sensor	632.8	TiO_2 - Ag - $BaTiO_3$	399.45	0.4606	183.99

CONCLUSION

According to the results of the theoretical analysis of the proposed SPR sensor performance, the SPR sensor improved sensitivity and figure of merits by 50.98 % and 13.93 %, respectively, over the convectional SPR sensor. The improvement in the sensor performance was due to the addition of optimized thickness of TiO_2 and $BaTiO_3$. Also, it measures water quality contamination with bacteria, and multiple heavy metal ions without any mechanical scanning. As a result of obviating mechanical scanning measuring time and error reduced. Furthermore, in terms of working SPR sensor performance, it outperforms the most recently published scientific article.

ACKNOWLEDGEMENTS

The authors would like to thank the Dar es Salaam Institute of Technology (DIT) for supporting this study.

REFERENCES

[1] Organization, W., *Tanzania's water and sanitation crisis*. 2022.

[2] Machiwa, J.F., *Heavy metal content in coastal sediments off Dar es Salaam, Tanzania.* Environment International, 1992. **18**(4): p. 409-415.

[3] Al–Rekabi, S.H., A. Al-Wahib, and M.J. Sharba. *The Use of Nanocomposite Au/Fe2H2O4–GO Based on Surface Plasmon Resonance to Detect Toxic Arsenic (V) in Aqueous Solution*. in IOP Conference Series: Materials Science and Engineering. 2019

[4] Sadrolhosseini, A.R., M. Naseri, and S.A. Rashid, *Polypyrrole-chitosan/nickel-ferrite nanoparticle composite layer for detecting heavy metal ions using surface plasmon resonance technique*. Optics & Laser Technology, 2017. 93: p. 216-223.. IOP Publishing.

[5] Invest, T., *Industrialization*. 2023. p. https://www.tanzaniainvest.com/industrialisation.

[6] Skoog, D.A., F.J. Holler, and S.R. Crouch, *Principles of instrumental analysis*. 2017: Cengage learning.

Article DOI: https://doi.org/10.37284/eaje.7.1.1967

[7] Taylor, H.E., Inductively coupled plasma-mass spectrometry: practices and techniques. 2001: Academic press.

[8] Mena, M., et al., Microcolumn preconcentration and gas chromatography-microwave induced plasma-atomic emission spectrometry (GC-MIP-AES) for mercury speciation in waters. Fresenius' journal of analytical chemistry, 1995. **351**: p. 456-460.

[9] Gao, Y., et al., Direct determination of mercury in cosmetic samples by isotope dilution inductively coupled plasma mass spectrometry after dissolution with formic acid. Analytica chimica acta, 2014. **812**: p. 6-11.

[10] Abdi, M.M., et al., Plasmonic Conducting Polymers for Heavy Metal Sensing, in Plasmonics-Principles and Applications. 2012, IntechOpen.

[11] Kumar, B.N., et al., Spectrophotometric determination of nickel (II) in waters and soils: Novel chelating agents and their biological applications supported by DFT method. Karbala International Journal of Modern Science, 2016. **2**(4): p. 239-250.

[12] Nogami, T., M. Hashimoto, and K. Tsukagoshi, Metal ion analysis using microchip CE with chemiluminescence detection based on 1, 10-phenanthroline–hydrogen peroxide reaction. Journal of separation science, 2009. **32**(3): p. 408-412.

[13] Wu, Z., et al., *Synthesis of mesoporous NiO nanosheet and its application on mercury (II) sensor*. Journal of Solid State Electrochemistry, 2012. **16**: p. 3171-3177.

[14] Mudgal, N., et al., BaTiO 3-graphene-affinity layer–based surface plasmon resonance (SPR) biosensor for pseudomonas bacterial detection. Plasmonics, 2020. **15**: p. 1221-1229.

[15] Kushwaha, A.S., et al., Zinc oxide, gold and graphene-based surface plasmon resonance (SPR) biosensor for detection of pseudomonas like bacteria: A comparative study. Optik, 2018. **172**: p. 697-707.

[16] Pandey, P.S., et al., SPR based biosensing chip for COVID-19 diagnosis-A review. IEEE Sensors Journal, 2022.

[17] Zainuddin, N.H., et al., Detection of adulterated honey by surface plasmon resonance optical sensor. Optik, 2018. **168**: p. 134-139.

[18] Jaafar, M., et al. Investigation of SU-8 as protection layer for prism SPR sensor towards reusable honey adulteration detection. in 2021 IEEE International Conference on Sensors and Nanotechnology (SENNANO). 2021. IEEE.

[19] Singh, S.K., A. Srivastava, and L. Dwivedi. A Theoretical analysis of Milk adulteration/contamination detection in camel, buffalo and cow milk using SPR Technique. in Journal of Physics: Conference Series. 2023. IOP Publishing.

[20] Haasnoot, W., G.R. Marchesini, and K. Koopal, *Spreeta-based biosensor immunoassays to detect fraudulent adulteration in milk and milk powder*. Journal of AOAC International, 2006. **89**(3): p. 849-855.

[21] Sharma, S., et al., *Investigation of Adulteration in Milk using Surface Plasmon Resonance*. ECS Journal of Solid State Science and Technology, 2021. **10**(9): p. 091004.

[22] Kumar, M. and S.K. Raghuwanshi. Design and analysis of surface plasmon resonance (SPR) sensor to check the quality of food from adulteration. in Physics and Simulation of Optoelectronic Devices XXVI. 2018. SPIE.

[23] Fen, Y.W., W.M.M. Yunus, and Z.A. Talib, Analysis of Pb (II) ion sensing by crosslinked chitosan thin film using surface plasmon resonance spectroscopy. Optik, 2013. **124**(2): p. 126-133.

Article DOI: https://doi.org/10.37284/eaje.7.1.1967

[24] Şolomonea, B.-G., et al., Cadmium ions' trace-level detection using a portable fiber optic—surface plasmon resonance sensor. Biosensors, 2022. **12**(8): p. 573.

[25] Wing Fen, Y. and W. Mahmood Mat Yunus, Surface plasmon resonance spectroscopy as an alternative for sensing heavy metal ions: A review. Sensor Review, 2013. **33**(4): p. 305-314.

[26] Verma, R. and B.D. Gupta, Detection of heavy metal ions in contaminated water by surface plasmon resonance based optical fibre sensor using conducting polymer and chitosan. Food chemistry, 2015. **166**: p. 568-575.

[27] Fen, Y.W. and W.M.M. Yunus, Characterization of the optical properties of heavy metal ions using surface plasmon resonance technique. Opt. Photonics J, 2011. **1**(03): p. 116-123.

[28] Daniyal, M., et al., Development of Surface Plasmon Resonance Spectroscopy for Metal Ion Detection. Sensors & Materials, 2018. **30**(9).

[29] 2Maurya, J.B. and Y.K. Prajapati, *Influence of adhesion layer on performance of surface plasmon resonance sensor*. IET Optoelectronics, 2018. **12**(4): p. 168-175.

[30] Chen, W. and J. Chen, Use of surface plasma waves for determination of the thickness and optical constants of thin metallic films. JOSA, 1981. **71**(2): p. 189-191.

[31] Meng, Q.-Q., et al., Performance analysis of surface plasmon resonance sensor with high-order absentee layer. Chinese Physics B, 2017. **26**(12): p. 124213.

[32] Chah, S., J. Yi, and R.N. Zare, *Surface plasmon resonance analysis of aqueous mercuric ions.* Sensors and Actuators B: Chemical, 2004. **99**(2): p. 216-222.

[33] Shalabney, A. and I. Abdulhalim, Electromagnetic fields distribution in multilayer thin film structures and the origin of sensitivity enhancement in surface plasmon resonance sensors. Sensors and Actuators A: Physical, 2010. **159**(1): p. 24-32.

[34] Hakami, J., A. Abassi, and A. Dhibi, Performance enhancement of surface plasmon resonance sensor based on Ag-TiO2-MAPbX3-graphene for the detection of glucose in water. Optical and Quantum Electronics, 2021. **53**(4): p. 164.

[35] Ishtiak, K.M., S.-A. Imam, and Q.D. Khosru, BaTiO3-Blue Phosphorus/WS2 hybrid structure-based surface plasmon resonance biosensor with enhanced sensor performance for rapid bacterial detection. Results in Engineering, 2022. **16**: p. 100698.

[36] Varasteanu, P. and M. Kusko, A multi-objective optimization of 2D materials modified surface plasmon resonance (SPR) based sensors: An NSGA II approach. Applied Sciences, 2021. **11**(10): p. 4353.

[37] Sun, P., et al., Sensitivity enhancement of surface plasmon resonance biosensor based on graphene and barium titanate layers. Applied Surface Science, 2019. **475**: p. 342-347.

[38] Sathya, N., et al., Tuning and sensitivity improvement of bi-metallic structure-based surface plasmon resonance biosensor with 2-d ε-tin selenide nanosheets. Plasmonics, 2022. **17**(3): p. 1001-1008.

[39] Vasimalla, Y., H.S. Pradhan, and R.J. Pandya, Sensitivity enhancement of the SPR biosensor for Pseudomonas bacterial detection employing a silicon-barium titanate structure. Applied Optics, 2021. **60**(19): p. 5588-5598.

[40] Singh, S., et al., Design and Modelling of High-Performance Surface Plasmon Resonance Refractive Index Sensor Using BaTiO3, MXene and Nickel Hybrid Nanostructure. Plasmonics, 2022: p. 1-14.

